Talanta 174 (2017) 347–356

Contents lists available at ScienceDirect

Talanta

journal homepage: www.elsevier.com/locate/talanta

Procedures for precise measurements of $^{135}Cs/^{137}Cs$ atom ratios in environmental samples at extreme dynamic ranges and ultra-trace levels by thermal ionization mass spectrometry

James A. Dunne[a,b,*], David A. Richards[a,b], Hsin-Wei Chen[a,c]

[a] Bristol Isotope Group, University of Bristol, Bristol, UK
[b] School of Geographical Sciences, University of Bristol, University Road, BS8 1SS Bristol, UK
[c] Department of Earth Sciences, University of Bristol, Queen's Road, BS8 1RJ Bristol, UK

ARTICLE INFO

Keywords:
Radiocaesium
TIMS
Interferences
Scattered $^{133}Cs^+$

ABSTRACT

Determination of $^{135}Cs/^{137}Cs$ atom ratios has the potential to be a powerful tool for nuclear forensics and monitoring environmental processes. We present optimized chemical separation techniques and thermal ionization mass spectrometry (TIMS) protocols to obtain precise $^{135}Cs/^{137}Cs$ atom ratios for a range of environmental sample types. We use a combination of double AMP-PAN separation and Sr-spec resin column purification to yield excellent separation from the alkali metals (Rb separation factor > 600), which normally suppress ionization of Cs. A range of emission activators for the ionization of Cs were evaluated and glucose solution yielded the optimal combination of a stable Cs^+ beam, minimal low-temperature polyatomic interferences and improved ionization efficiency. Mass-spectrometric determination of low abundance ^{135}Cs and ^{137}Cs is compromised by the presence of a very large $^{133}Cs^+$ beam, which may be scattered and cause significant spectral interferences. These are explored using multi-static Faraday cup – ion counter methods and a range of energy filter settings. The method is evaluated using environmental samples and standards from regions affected by fallout from Chernobyl (IAEA-330) and Fukushima nuclear disasters. Where the intensity of $^{133}Cs^+$ is large relative to $^{135}Cs^+$ and $^{137}Cs^+$ (< 30 cps), minor polyatomic interferences need to be considered. In the absence of a standard with $^{135,\ 137}Cs/^{133}Cs < 1 \times 10^{-8}$, we explored the reproducibility of $^{135}Cs/^{137}Cs$ atom ratios at these high dynamic ranges and extremely low abundance ($^{137}Cs \approx 12$ fg g^{-1}) for sediments from an estuarine setting in SW England, UK.

1. Introduction

Radiocaesium has been widely dispersed across the Earth due to nuclear operations since the first atmospheric nuclear weapons test in 1945 [1–4]. Caesium has a strong affinity for particulates, which makes it a powerful tracer for a range of environmental processes [5–9]. Conventionally, ^{137}Cs is routinely monitored in sediments, aerosols, plants etc. by gamma-spectrometry, but rarely are all of the high-yield Cs fission and activation products measured. The continual release, remobilization and dispersion of ^{137}Cs in the environment enhances mixing of ^{137}Cs from different sources causing background quantities to increase. Where multiple sources of ^{137}Cs are associated with an environmental deposit, it is important that we consider the additional Cs isotopes to determine provenance and pathway [10–13]. While source terms may be identified by quantifying $^{134}Cs/^{137}Cs$ activity ratios using gamma-spectrometry [14–18] this approach is limited because of the short half-life of ^{134}Cs (2.07 a).

One can also turn to the much-longer lived radiocaesium isotope, the low energy β-emitter, ^{135}Cs ($t_{1/2}$ = 2.3 Ma). While the specific activity is much less than that of $^{134,\ 137}Cs$, limiting the use of radiometric techniques, its atomic abundance is suitable for mass spectrometric determination. Although the low decay energy eliminates this nuclide from being an immediate radiological risk, its long half-life and high fission yield have caused it to be identified as a major contributor to radiological risk for geological disposal/storage facilities [19,20]. Furthermore, because of the large neutron capture cross-section its parent nuclide, ^{135}Xe, the production of ^{135}Cs relative to ^{136}Xe is a function of neutron flux and the reactor conditions that govern ^{135}Xe concentration (Fig. A1). These characteristics cause $^{135}Cs/^{137}Cs$ to be an extremely sensitive reactor proxy for nuclear forensics, nuclear waste characterization and tracing environmental processes [11,21–23].

Measurement of $^{135}Cs/^{137}Cs$ was addressed initially by Lee et al. [24], using thermal ionization mass spectrometry (TIMS). However,

* Corresponding author at: Bristol Isotope Group, University of Bristol, Bristol, UK.
E-mail address: james.dunne@bristol.ac.uk (J.A. Dunne).

http://dx.doi.org/10.1016/j.talanta.2017.06.033
Received 14 April 2017; Received in revised form 7 June 2017; Accepted 12 June 2017
Available online 13 June 2017

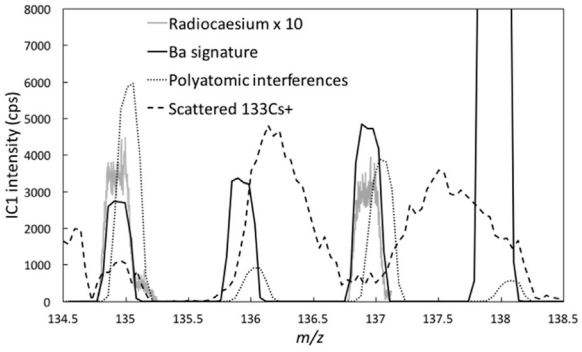

Fig. 1. Superimposed mass scans of radiocaesium and potential interferences that may occur from *m/z* 134.5 – 138.5.

due to the associated analytical challenges, only a few laboratories have published $^{135}Cs/^{137}Cs$ data for environmental samples such as water, sediments and vegetation [10–12,22–32]. Challenges are caused by the low abundance of radiocaesium in environmental samples relative to problematic matrix components such as, $^{134, 135, 137}Ba$ and ^{133}Cs, that are present in far greater quantities (Fig. 1) [24,33]. Here we optimize ionization conditions whilst taking advantage of the *m/z* filtering capability of TIMS to build on the achievements of others [24,26].

One of the principal challenges is the elimination of Ba as an isobaric interference. Resistive heating of a Re filament and suitable activator can be used to selectively ionize Cs at low temperatures without promoting Ba ionization. This approach permits the measurement of Cs isotopes in the presence of residual trace Ba (0.7 – 5 ng L^{-1}) after separation chemistry or in reagent blanks: to completely remove Ba is extremely challenging [33]. While eliminating the need to correct for Ba interferences reduces one component of measurement uncertainty, it does introduce minor considerations including, (1) incomplete separation of Cs from other elements, such as alkali metals, that can suppress Cs ionization, (2) while activators can be used to optimize ionization behavior, they may also introduce polyatomic interferences. In addition, measurement of low abundance radiocaesium peaks in the presence of extremely large, natural $^{133}Cs^+$ beams requires careful consideration for scattered ions and tailing.

In this paper, we investigate how different chemical treatment procedures may be used to provide information on the partitioning of natural and anthropogenic caesium in environmental samples and also their effect on potentially contaminating elements. The behavior of Rb and Cs with AMP-PAN and Sr-spec resin are explored and the effect of their separation on TIMS analysis is discussed. We assess the influence of different activators on Cs ionization efficiency and problematic interferences. The *m/z* filtering capabilities of TIMS for extremely high-dynamic range measurements, with consideration for detector preservation and scattered ions, are explored. These findings are assimilated to produce a robust, routinely-applicable method for the determination of fallout radiocaesium in a range of environmental samples, most notably, estuarine sediments. The proposed methodology is evaluated using environmental samples contaminated by the Fukushima Daiichi Nuclear Power Plant and Chernobyl disasters.

2. Materials and methods

Rb/Cs concentration ratio is referred to as a proxy for Cs separation throughout this paper. Because Rb behaves extremely similarly to Cs, separation of Cs from Rb is expected to be indicative of successful separation of Cs from other problematic matrix components.

2.1. Instrumentation

All concentration measurements were performed using a ThermoELEMENT 2XR sector field-inductively coupled plasma mass spectrometer (SF-ICPMS). Prior to conducting measurements, the instrument was tuned and a mass calibration was performed. Stable Cs and Rb concentration standards were prepared from 1 g L^{-1} elemental stock solutions (Sigma-Aldrich, Steinheim, Germany).

Isotopic analyses were conducted using a ThermoFinnigan Triton TIMS. The instruments detector system is equipped with 8 moveable Faraday cups and a fixed center cup or SEM. The SEM is positioned behind a retarding potential quadrupole (RPQ). Standard purity Re single filaments were used for all measurements.

2.2. Pretreatment: selective leaching to minimize Rb/Cs

Approximately, 0.5 g of Severn Estuary sediment was dry ashed at 450 °C for 12 h, pulverized and transferred to a polytetrafluoroethylene (PTFE) vial (Savillex, Minnetonka, USA). Nitric acid leaches (10 mL) were performed at range of concentrations (0.5–12 M) and a complete acid digest was also conducted using 6 mL 16 M HNO_3 and 3 mL 28 M HF (All reagents used were analytical grade or purer). The samples were left to reflux at 165 °C for 12 h before Cs and Rb concentrations were determined by SF-ICPMS.

2.3. Pretreatment: preferential extraction of radiocaesium from ^{133}Cs

To increase $^{135, 137}Cs/^{133}Cs$ by sample pre-treatment, a 1 M HNO_3 leach was compared to an 8 M HNO_3 leach. This experiment was performed on homogenized sediment (1 g), sampled from the Esk Estuary, Cumbria. The site has sequestered radiocaesium introduced to the Irish Sea by Sellafield Nuclear Reprocessing Plant over the last 50 years [34,35]. The respective leachates underwent chemical separation prior to isotopic analysis by TIMS.

2.4. Separation of alkali metals from matrix components

Initial pre-concentration was performed by placing 1 mL of AMP-PAN resin into a BioRad 30 × 80 mm Econo-Pac column. The resin was pre-conditioned with 10 mL 18 MΩ H_2O, followed by 10 mL 3.5 M HNO_3. Sample was loaded onto the column in 2 mL 3.5 M HNO_3, rinsed with 20 mL 0.2 M NH_4NO_3 and 10 mL 18 MΩ H_2O, the Cs was subsequently eluted with 4.8 mL 5% (v/v) NH_4OH followed by 7.2 mL 18 MΩ H_2O. Recovery of Cs from AMP causes the material to decompose introducing Mo to the eluent. Here, solution should be kept in basic conditions to prevent the formation of insoluble molybdate complexes, $M^{X+}(MoO_4^{2-})_X$ [36,37]. To separate Cs from Mo, ~ 20 mL of anion exchange resin (BioRad AG1-X8, OH^- form, 200 – 400 mesh), was loaded into a 30×80 mm column, preconditioned with 20 mL 18 MΩ H_2O and 20 mL 2.5% (v/v) NH_4OH, before loading the sample. The resin retains Mo while Cs was collected immediately. Smaller volumes of resin did not sufficiently remove Mo leaving insoluble residue that retained Cs when the eluent was dried down. Ammonium salts were removed by refluxing the sample in 1 mL 16 M HNO_3 and 1 mL 30% (v/v) H_2O_2 at 165 °C for 4 h before allowing the solution to evaporate. The sample was dissolved in 2 mL 3.5 M HNO_3.

2.5. Separation of Cs^+ from the other alkali metals

For further separation, 1 mL of AMP-PAN was placed in a 4 × 50 mm STFE column (Shrinktec polymers international) and conditioned with 10 mL 18 MΩ H_2O, followed by 10 mL 3.5 M HNO_3. Sample was loaded onto the column and rinsed with 15 mL 0.2 M NH_4NO_3, which selectively exchanges K^+ and Na^+ with NH_4^+. The greater abundance of matrix components, specifically cations, are anticipated to inhibit this exchange step during the pre-concentration stage. The resin was then rinsed with 3 M NH_4NO_3 to elute Rb while Cs is retained. Elution profiles for 3 homogenized environmental samples (estuarine silts from Severn Estuary, UK) were determined using SF-ICPMS to quantify Cs loss and Rb removal. Prior to elution, the resin

should be rinsed with 15 mL 18 MΩ H_2O to ensure NH_4NO_3 is not introduced to the eluent fraction. Sample was eluted with 4.8 mL 5% (v/v) NH_4OH and 7.2 mL 18 MΩ H_2O. The same anion exchange and oxidation steps were performed to remove Mo and ammonium salts.

2.6. Final purification of Cs^+ from Rb^+

Samples from the previous step were adjusted to 1 mL 1 M HNO_3 and loaded onto 1 mL of Sr-spec resin in a 4 × 50 mm STFE column preconditioned with 10 mL MΩ H_2O and 10 mL 1 M HNO_3. The Cs fraction was collected immediately, Rb/Cs was subsequently determined by SF-ICPMS.

2.7. Comparison of activators for desired Cs ionization

To quantify ionization efficiencies for the following activators, tantalum chloride in phosphoric acid, silica gel mixed with phosphoric acid and glucose solution, the same activator was applied to 3 filaments. Increasing quantities, 1 ng, 10 ng and 100 ng, of ^{133}Cs were subsequently loaded onto the activator-coated filaments. This experiment was also performed on a filament with no activator.

2.8. Assessing the effect of detector configuration on scattered $^{133}Cs^+$

To illustrate scattering of $^{133}Cs^+$, a series of mass scans were performed where Faraday cups L1 and L2 were moved across the focal plane while *m/z* 134.5 – 139.0 were focused into the axial SEM (Fig. A3). This was performed by loading 1 μg ^{133}Cs with glucose activator onto a single, standard purity Re filament. To quantify these effects, measurements of an internal radiocaesium standard were conducted under two scenarios (1) *m/z* 134.905 and *m/z* 136.905 (atomic mass units of ^{135}Cs and ^{137}Cs, respectively), were counted on the axial SEM while $^{133}Cs^+$ was simultaneously collected in a Faraday cup. (2) *m/z* 134.905 and *m/z* 136.905, were counted on the axial SEM with no $^{133}Cs^+$ collection. For both of these experiments, ions were detected after passage through the Retarding Potential Quadrupole (RPQ) filter, which filters ions based on energy and angle of trajectory.

2.9. Changing RPQ filter settings to consider behavior of scattered $^{133}Cs^+$

For these experiments, 1 μg ^{133}Cs was loaded onto a Re filament with glucose activator. Mass scans for *m/z* 134.5 – 139 were performed with a large $^{133}Cs^+$ beam (30 – 40 V). Between measurements, RPQ settings for suppressor and deflection voltages were adjusted from standard settings (2740 V and 9954 V, respectively) to extreme potentials that, theoretically, prevent ion transmission to the SEM (0 V and 9974 V, respectively).

2.10. Minimising the exposure of Faraday cups to large $^{133}Cs^+$ beams

To avoid exposing multiple Faraday cups to large $^{133}Cs^+$ beams, Faraday cup L2 was moved across the focal plane between measurements: firstly $^{135}Cs(IC1)/^{133}Cs(L2)$ was quantified, then Faraday cup L2 was moved across the focal plane to measure $^{137}Cs(IC1)/^{133}Cs(L2)$. To evaluate this measurement technique, it was compared to a peak jumping method using Faraday cups L2 and L1. This experiment was performed using a radiocaesium sample where $^{135,\ 137}Cs/^{133}Cs \approx 1 \times 10^{-7}$.

2.11. Evaluation of methodology

To evaluate the methodology, reference material IAEA-330 (spinach) was obtained from the International Atomic Energy Agency (IAEA) and environmental samples were collected from areas of the Japanese environment that have been heavily contaminated by the Fukushima Daichii Nuclear Power Plant disaster. Finally, to assess this methodology for estuarine samples, where $^{135,\ 137}Cs/^{133}Cs$ is on the order of 1×10^{-9}, a 40 Bq kg^{-1} (12 fg g^{-1}) estuarine sediment sample (quantified by gamma-spectrometry) was collected from the Severn Estuary, homogenized and split into 3, 1 g sub-samples.

3. Results and discussion

3.1. Recommendations for chemical separation

The presence of alkali metals suppresses the ionization of Cs [38]. Inadequate chemical separation of Cs from the other alkali metals causes it to ionize at the same temperatures as Ba. The high abundance of these metals in estuarine sediments relative to Cs, combined with their similarities in chemical behavior makes this separation extremely challenging.

Recently, Snow et al. compared three different purification steps following initial pre-concentration by AMP-PAN [26]. Further purification by AMP-PAN cation exchange followed by anion exchange and a final micro-cation exchange step provided the greatest separation from Rb. Subsequent publications demonstrate that this is a robust method for measuring ultra-trace quantities of Cs isotopes in soils and vegetation by TIMS [11,22,25]. When this technique was applied to estuarine sediments - which are typically clays that contain high quantities of Rb in the mineral matrix and also, due to the nature of the marine environment, contain considerably higher concentrations of alkali metals - it was not possible to obtain a consistent elution profile for the final micro-cation exchange step. Furthermore, commercial cation-exchange resins have low selectivity over similar cations such as the alkali metals, particularly Rb and Cs [39]. To account for these inherently complex matrix effects, modifications have been made to sample pre-treatment, the AMP-PAN cation-exchange step and rather than purifying by microcation exchange, Sr spec resin (Triskem International) has been examined for the final separation step. It should be highlighted that AMP-PAN is a relatively new separation material highly selective towards Cs which, following decomposition, if the eluent is not kept in appropriate chemical conditions, can form an insoluble substrate, compromising the respective sample. For these reasons, it is prudent to continue efforts in optimizing the analytical procedures associated with this material.

3.1.1. Pretreatment: selective leaching to minimize Rb/Cs

Complete acid digest yielded Rb/Cs = 15.0 ± 3.1. Fig. 2 indicates that HNO_3 molarities between 4 M and 12 M yield the lowest Rb/Cs (~ 11). A concentration of 7 M HNO_3 was selected for routine work to ensure residual organics from ashing decompose. Higher concentrations were avoided to minimize the addition of other undesirable species to the system with similar chemical properties to Cs^+, such as Zn^{2+} [40]. These data demonstrate how specialized sample pretreatment protocols may be implemented to simplify subsequent separation chemistry.

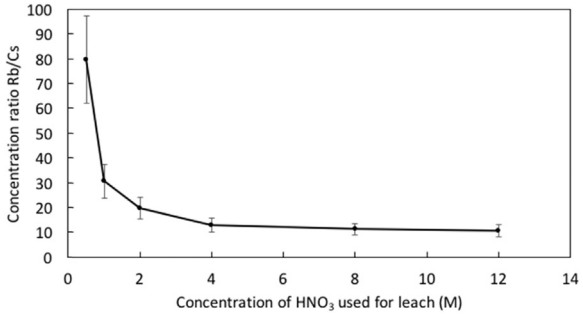

Fig. 2. Concentration ratios of Rb/Cs leached from estuarine sediment by nitric acid at a range of concentrations. Uncertainties estimated to 2σ.

Table 1
Comparison of atom ratios for two acid leaches performed on the same homogenized estuarine sediment sample. Uncertainties are presented to 2 SE.

HNO_3 used for leach (M)	$^{135}Cs/^{133}Cs$	$^{137}Cs/^{133}Cs$	$^{135}Cs/^{137}Cs$
8	$1.82 (\pm 0.06) \times 10^{-8}$	$1.04 (\pm 0.04) \times 10^{-8}$	1.76 ± 0.06
1	$1.09 (\pm 0.02) \times 10^{-7}$	$6.21 (\pm 0.17) \times 10^{-8}$	1.75 ± 0.06

3.1.2. Pretreatment: preferential extraction of radiocaesium from ^{133}Cs

The experiments performed here demonstrate 1 M HNO_3 leaches produce larger $^{135,\ 137}Cs/^{133}Cs$ in comparison to treatment with 8 M HNO_3 (Table 1). The 1 M leach increases $^{135,\ 137}Cs/^{133}Cs$, by ~ 80% without altering $^{135}Cs/^{137}Cs$. Although, $^{135,\ 137}Cs/^{133}Cs = 1 \times 10^{-8}$ still induces $^{133}Cs^+$ scattering, scattering will be reduced. This will improve precision and preserve Faraday cups from large $^{133}Cs^+$ beams. We advise this technique is used with discretion for samples that have received multiple sources of radiocaesium: this technique may selectively extract one source of radiocaesium without extracting others [41].

The possibility of extracting different components of radiocaesium is a key advantage: Preliminary findings suggest selective extractants may be used to liberate specific sources of radiocaesium partitioned within different geochemical fractions of an environmental sample. Using selective pre-treatments to extract multiple, isotopically distinct sources associated with the same environmental sample would provide the opportunity to more accurately ascertain source attribution and to interpret, in greater depth, the conditions that led to the production of the radiocaesium. Specifically, pretreatment in this way may be implemented to separate the fraction of an isotopic system associated with a given release event while global fallout material is retained on the material. This tactic could be employed to permit interpretation of an isotope ratio that may otherwise be compromised by mixing with global fallout material. Environmental samples from the Fukushima prefecture are an example of a recent scenario where global fallout has obstructed interpretation in this way [22]. It must be acknowledged, however, that while this approach demonstrates potential, for samples where Cs is in a refractory phase, such as a fuel cladding particle associated with moss, total digestion procedures will be necessary [42].

3.1.3. Separation of Rb from Cs by AMP-PAN

While the presented elution profile is expected to be sensitive to variations in sample matrix composition and column parameters, calibrations for 3 replicates of homogenized estuarine sediment show that rinsing with excess amounts of NH_4NO_3 can prematurely elute Cs considerably reducing yield (Fig. 3). Surprisingly, this occurred without the typical colour change that is caused by the decomposition of AMP from PAN, suggesting Cs was eluted without the introduction of large quantities of Mo. Based on these observations, for routine work on estuarine sediments, the prescribed addition of 10 mL 3 M NH_4NO_3 was adjusted to 5 mL. Additionally, it highlights this step should be well-calibrated for the respective sample and column parameters. This step reduced Rb/Cs to ~ 0.6, however, further separation from Rb was necessary to lower the Cs ionization temperature from Ba ionization.

3.1.4. Final purification of Rb^+ from Cs^+ by Sr-spec resin

To further purify Rb from Cs, a Sr-spec resin column was used in place of the previously recommended micro-cation exchange column [26]. Sr-spec resin has previously been used to purify from Cs^+ from Ba^{2+} [32,33]. However, the chemical properties of Rb and Cs are more similar, and the potential of Sr-spec resin to purify Cs^+ from Rb^+ for environmental applications has not yet been examined. The Sr-spec column improved Cs separation from Rb: Rb/Cs ≈ 0.04 (Table 2). In combination with the appropriate activator (discussed in Section 3.4),

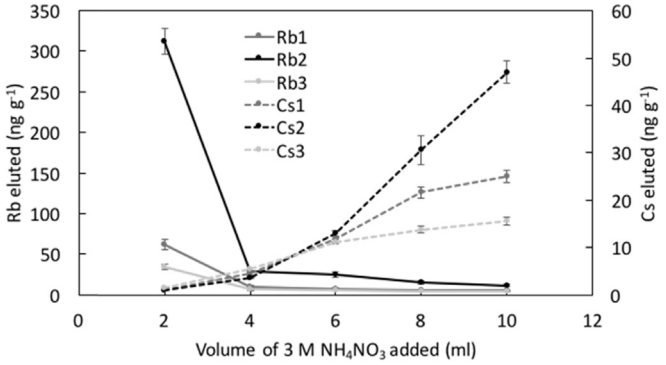

Fig. 3. Elution profile of Rb and Cs for 3 replicates of homogenized estuarine sediment. Uncertainties estimated to 2SE.

this degree of separation adequately reduced the ionization temperature of Cs to ~ 750 °C, resolving the issue of trace Ba impurities as isobaric interferences. Furthermore, extraction chromatography eliminates the requirement of, potentially labor intensive, column calibrations. Eliminating the requirement of column calibration also improves the robustness of chemical separation because the system will not require recalibration for different sample matrices [26].

3.2. Comparison of activators

A stable ion beam is required to conduct accurate and precise measurements. This requires a reagent that optimizes the thermochemical properties of Cs for a given filament configuration. This must be achieved without promoting the ionization of other (polyatomic) interferences.

Other studies have increased the ionization efficiency of Cs using an ion cavity source and a triple filament configuration [26,43]. To avoid making non-trivial modifications to the ion source, several activators have been evaluated to promote ionization using a single filament configuration. In promoting the ionization of an analyte at low temperatures (≤ 900 °C), several activators also promoted ionization of polyatomic interferences that otherwise decompose at the more typical, higher temperatures of ionization (> 1500 °C), despite implementing extensive filament cleaning and degassing procedures. Such species are also observed elsewhere [23,24,26,44]. The behavior of these low-temperature polyatomic interferences are investigated and a suitable activator is recommended. Increasing ionization efficiency without yielding interfering species can considerably improve precision. Additionally, such information is expected to be beneficial for the analysis of other species that are ionized at comparatively low temperatures (700 – 1100 °C) such as Li, B and Os.

For a single filament configuration, loading the sample with an activator to improve ionization efficiency and stabilize the Cs^+ beam was essential to conduct measurements (Table 3). Activators were selected for testing based on the following rationale:

Table 2
Comparison of Rb separation factors for procedures following initial pre-concentration.

Study	Method (following initial pre-concentration by AMP-PAN)	Rb separation factor
Snow et al. [26]	Cation Exchange	2.2
	AMP-PAN	> 100
This study	Cation exchange	2.3
	Sr-spec	110
	AMP-PAN	20
	Additional AMP-PAN separation followed by Sr-spec	> 600

Table 3
Ionization efficiency (%) of activators tested for optimal ^{133}Cs ionization.

Activator	Quantity of ^{133}Cs loaded (ng)		
	1	10	100
None	2.30×10^{-2}	2.30×10^{-3}	2.44×10^{-5}
Silica gel + H_3PO_4	4.16	6.55	17.52
$TaCl_5$ + H_3PO_4	7.66	11.73	7.12
Glucose	5.45	7.02	5.60

- Tantalum chloride in phosphoric acid was examined because it is routinely used for the analysis of Sr isotopes by TIMS [45,46]. It was anticipated this activator would be suitable for Cs given that Sr has the most similar ionization properties to Cs in the periodic table out of the elements routinely measured by TIMS.
- Silica gel mixed with phosphoric acid: silica gel forms a molten glass across the filament surface, it was hypothesized this may suppress the emission of polyatomic interferences [47].
- Although not reported, a glucose activator has successfully been implemented elsewhere to promote Cs ionization [23,24].

Observations of the discussed interferences showed inconsistent *m/z* 135/*m/z* 137, indicating the interferences are not isobaric because they do not exhibit the isotopic signature of Ba (the only element with nuclides at isobars 135 and 137). Additionally, the respective interferences did not exhibit the same isobaric constituents that occur at different isobars as they do not share the same ionization behavior e.g. identical molecules that vary by 2 mass units due to an isotopic constituent with a mass that also varies by 2 mass units, such as $^{123}Sb^{14}N$ and $^{121}Sb^{14}N$. Based on these observations, it is apparent the respective interferences are multiple polyatomic species, and given their unpredictable ionization behavior, do not demonstrate characteristics that allow for correction.

A mixture of TaCl and H_3PO_4 consistently yielded the greatest intensity of polyatomic interferences (> 1000 cps), while the silica gel and H_3PO_4 suppressed their intensity to < 50 cps. Even at this relatively low background, the inconsistent nature, both temporally and from sample to sample (although variation from sample to sample may be a function of source lens tuning), meant that they could not be accurately corrected for. In considering this behavior, these interferences resemble those described by Snow et al. [26], rather than the $NaRbCN^+$ interference reported by Lee et al. [24] and Chen et al. [23].

Glucose was examined as a potentially suitable activator. Applying glucose to the filament prior to loading the sample does not yield polyatomic interferences and therefore, was selected as a routine activator. To avoid carburization, which can cause sporadic ionization of the analyte and an unstable Cs^+ beam, only the thinnest layer of glucose should be applied. In removing the requirement of correcting for background interferences, analytical precision can be considerably improved. Additionally, by recommending an activator that increases ionization efficiency, in situations where sample quantity is limited, it is possible to achieve much greater precision.

3.3. Scattered $^{133}Cs^+$ as a spectral interference

If a large (> 20 V) $^{133}Cs^+$ beam is not focused into a Faraday cup, $^{133}Cs^+$ is scattered. This introduces spectral interferences on the axial SEM at *m/z* 134, 135 and 137 that increase as a function of beam intensity (Fig. 4). Considering Cs^+ is used as a sputter source, it is highly desirable not to collect intense $^{133}Cs^+$ beams in a Faraday cup to avoid unnecessarily damaging the detector.

Currently, the behavior of these unusual interferences is only briefly mentioned in the literature and does not appear to be well-understood [44]. Here, we perform novel experiments to assess the behavior of scattered $^{133}Cs^+$ with respect to detector geometry and the voltages applied to the retarding potential quadrupole (RPQ). We recommend techniques to minimize the detrimental effects of large $^{133}Cs^+$ beams on Faraday cups and demonstrate their validity. Constraining the *m/z* filtering capabilities of these instruments is crucial in undertaking high dynamic range experiments: for samples in this work $^{135, 137}Cs/^{133}Cs \approx 1 \times 10^{-9}$. Observations of Cs isotopes at high dynamic ranges are anticipated to be valuable for similar, high dynamic range isotopic measurements, such as $^{236}U/^{238}U$, $^{41}Ca/^{40}Ca$, $^{129}I/^{127}I$ and $^{90}Sr/^{88}Sr$ [48–51].

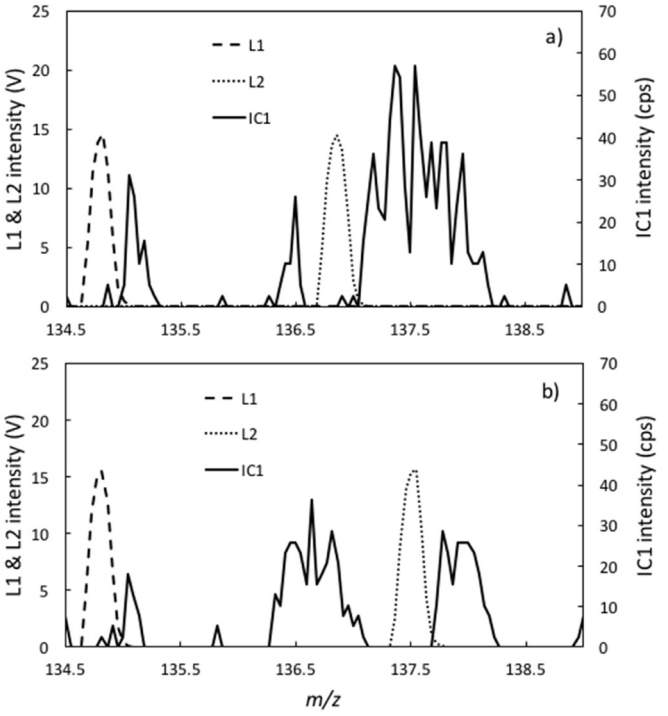

Fig. 4. Mass scans taken from *m/z* 134.5 – 139.0 where Faraday cup L1 is kept in the same position while L2 is positioned at a) *m/z* 136.91 and b) 137.50.

The effect of scattered $^{133}Cs^+$ on the background of *m/z* 134.905 and *m/z* 136.905 is provided below (Table 4). Evidently, the background increases by a factor of ~ 100 when $^{133}Cs^+$ is not collected in a Faraday cup, while collecting $^{133}Cs^+$ is likely to damage the respective cup.

3.3.1. The effect of Faraday cup position on scattered $^{133}Cs^+$

A mass scan is performed to qualitatively assess the abundance of species that are present over an *m/z* range of interest. In the case of the Triton TIMS used in this work, the voltage applied to the magnetic sector is adjusted to *swing* an ion beam across the focal plane. This incrementally focusses the ion beam into a detector before focusing a higher *m/z* into the same detector. In this way, a mass spectrum is obtained: a profile of the relative intensity of ionic species that occur over an *m/z* range of interest. Mass scans are typically performed to identify problematic interfering species or to screen a sample to determine the relative abundance of analytes.

Table 4
Comparison of background at *m/z* 134.905 and *m/z* 136.905 where either $^{133}Cs^+$ is focused into Faraday cup L2 or $^{133}Cs^+$ is not collected. Uncertainties estimated to 2 SE.

Cup position	No collection of $^{133}Cs^+$	$^{133}Cs^+$ collected in L2
Integration time (s)	2.1	2.1
No. of cycles	30	30
$^{133}Cs^+$ intensity (V)	24	25
m/z 133.905/^{133}Cs	–	$3.97 (\pm 0.15) \times 10^{-9}$
m/z 134.905/^{133}Cs	$2.22 (\pm 0.24) \times 10^{-9}$	$1.23 (\pm 0.71) \times 10^{-11}$
m/z 136.905/^{133}Cs	$1.75 (\pm 0.15) \times 10^{-9}$	$2.57 (\pm 1.44) \times 10^{-11}$

For the low $^{135,\ 137}Cs/^{133}Cs$ samples investigated in this work, it is necessary to perform mass scans at *m/z* 134.5 – 139.0 to ensure interferences do not affect measurements. However, while *m/z* 134.5 – 139.0 is focused into the SEM, the extremely large $^{133}Cs^+$ beam is moved across the back of the detector system. Off-axis Faraday cups on the low mass side of the SEM may be positioned to instantaneously capture the $^{133}Cs^+$ beam while a given *m/z* is quantified by the SEM. However, for periods where the large $^{133}Cs^+$ beam is not collected in a Faraday cup, and therefore focused into the back of the detector system, we demonstrate $^{133}Cs^+$ may be scattered in such a way that it it creates an artificial trace at *m/z* (134.5 – 139). This is illustrated by the ~ 40 cps at *m/z* 137.5 in Fig. 4a that is removed when L2 is moved from *m/z* 136.9 to *m/z* 137.5 (Fig. 4b).

To obtain a mass spectrum "clean" of scattered $^{133}Cs^+$, a series of mass scans have been performed where a Faraday cup is sequentially moved across the focal plane (Fig. A3). This approach captures the entire *m/z* range of interest without producing scattered $^{133}Cs^+$. This seems to be the only means of exploring the non-scattered components of a mass spectrum. These scans also demonstrate that the scattered $^{133}Cs^+$ profile changes as a function of detector geometry, suggesting that the direction of scattering is affected by the position of the off-axis Faraday cups.

A comparison of $^{135}Cs/^{137}Cs$ measurements show that there appears to be an inaccurate shift 10% – 15% when $^{133}Cs^+$ is not collected in a Faraday cup (Fig. 5). Considering this shift is quite subtle, and the $^{135,\ 137}Cs/^{133}Cs$ remains constant with respect to time and Cs intensity, if mass scans are not conducted, it is unlikely spectral interferences will be identified. These measurements highlight the importance of collecting $^{133}Cs^+$, when performing high dynamic range measurements. To preserve Faraday cup L1, two cup configurations were compared (Table 5). The ratios obtained from the respective cup configurations are in good agreement with one another. We believe this is the most effective compromise, where Faraday cup L1 is preserved and $^{135}Cs/^{137}Cs$ atom ratios are accurately quantified.

3.3.2. Assessing the effect of RPQ lens voltages on scattered $^{133}Cs^+$

The scattering events that alter the *m/z* of $^{133}Cs^+$ reduce the ions energy and change their angle of trajectory. The RPQ is positioned in front of the axial ion counter and is designed to act as an extremely selective lens capable of filtering ions as a function of their direction and energy. Therefore, it is reasonable to expect the RPQ ion lenses to discriminate scattered species. To assess the *m/z* filtering capabilities of the RPQ on scattered $^{133}Cs^+$, the deflection and suppressor voltages were set to their extremes, 0 V and 9974 V, respectively. Theoretically, this should cause the deflection voltage to deflect all ions towards the central Faraday cup rather than the axial SEM and the suppression voltage to reduce transmission through the RPQ. Surprisingly, despite setting the deflection and suppressor voltages to their extremes, an IC1 trace similar to that of the characteristic scattered $^{133}Cs^+$ was observed (Fig. 6). Furthermore, increasing the suppressor voltage to 9974 V did not appear to alter the profile of the scattered $^{133}Cs^+$.

Possibilities for such behavior include leakage of scattered ions through the SEM side cover or detection of neutral species (J. Schweiters, pers. comm).

Considering that during these experiments, there are ~ 2×10^9 $^{133}Cs^+$ colliding with the back of the detector system each second, it seems feasible that 100 of these ions (200 ppb) may be scattered in such a geometry that causes them to pass through the spaces in the side cover of the SEM. Halicz et al. [52], experience similar issues with scattered $^{40}Ar^+$ and $^{40}Ca^+$ at *m/z's* around 40, when attempting high-precision measurements of Ca isotopes via MC-ICPMS. The interferences are attributed to the ions being scattering around the detector housing.

It is highly unlikely that neutral species could travel from source to detector, however, $^{133}Cs^+$ may generate neutral species in the detector housing capable of passing through ion lenses unperturbed. This scenario is comparable to secondary ionization mass spectrometry (SIMS) where neutrals tend to be the most abundant species generated.

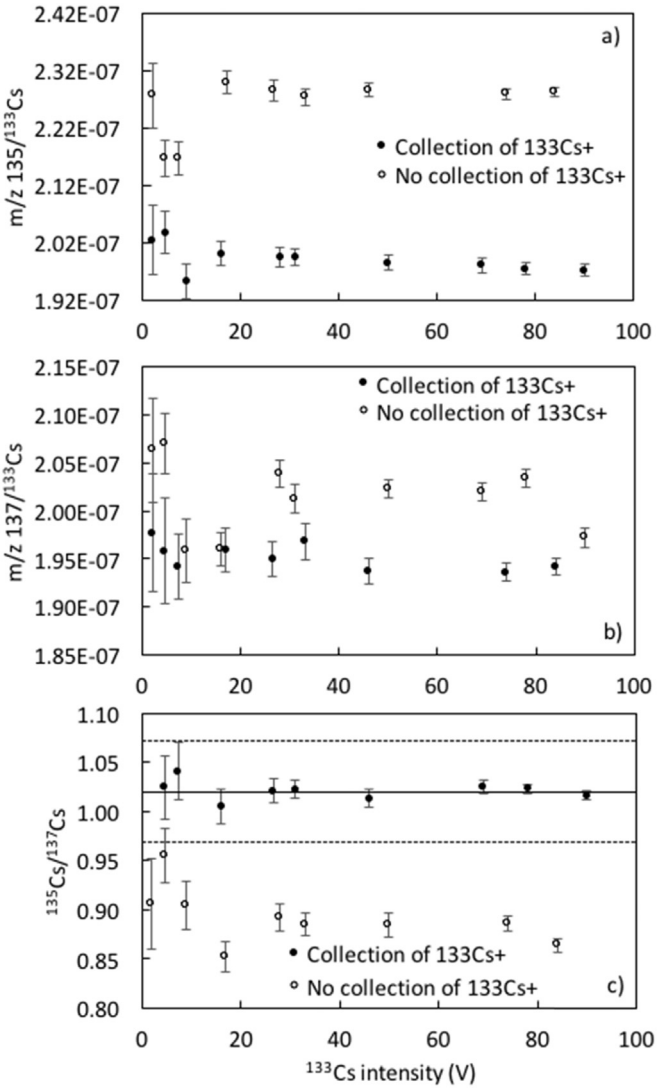

Fig. 5. The effect on $^{135}Cs/^{137}Cs$ atom ratio measurements when $^{133}Cs^+$ is collected in a Faraday cup. Repeat measurements have been performed on an internal radiocaesium standard loaded onto the same filament for **(a)** *m/z* 135/^{133}Cs and **(b)** *m/z* 137/^{133}Cs. **(c)** Represents the $^{135}Cs/^{137}Cs$ atom ratios calculated from (a) and (b). The solid line represents the average $^{135}Cs/^{137}Cs$ atom ratio where $^{133}Cs^+$ has been collected in a Faraday cup. The dashed lines are the respective 95% confidence intervals. Uncertainties are presented to 2SE.

Table 5
Comparison of peak-jumping via two Faraday cups to two separate methods where cup L1 is preserved and cup L2 is moved between the respective methods. Uncertainties are presented to 2SE.

Method	Cup configuration			$^{135}Cs/^{137}Cs$ atom ratio
	L2	L1	IC1	
1)	^{133}Cs	^{133}Cs	^{135}Cs ^{137}Cs	$0.616 \pm 3.342 \times 10^{-3}$
2)	^{133}Cs	moved away	^{135}Cs	$0.613 \pm 3.338 \times 10^{-3}$
3)	^{133}Cs	moved away	^{137}Cs	

3.4. Measurement of reference materials

There are no commercially available certified reference materials for the determination of $^{135}Cs/^{137}Cs$ atom ratios. Therefore, to evaluate this method, we have obtained environmental samples that have been exposed to the same release event as those values quoted elsewhere. A number of studies have compared IAEA-375; a soil sample collected

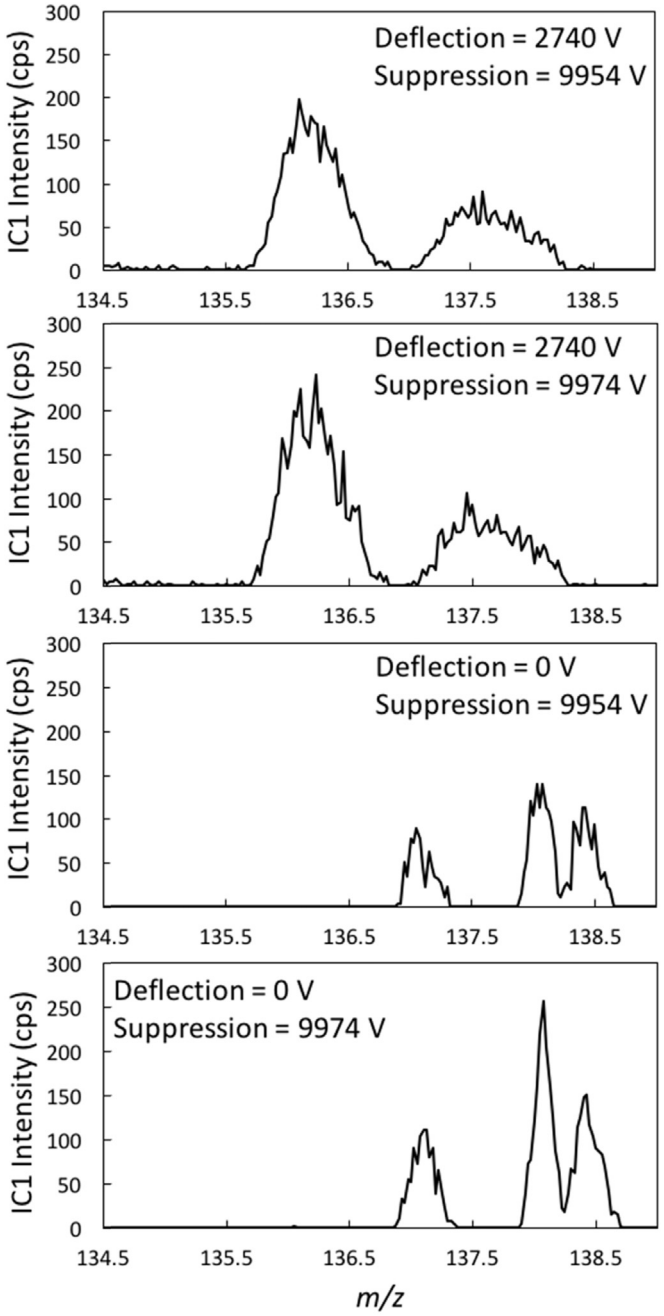

Fig. 6. Profiles of scattered $^{133}Cs^+$ from a 35 V $^{133}Cs^+$ beam following changes made to RPQ settings.

from Novozybkov, Russia contaminated from the Chernobyl disaster of 1986 [12,26,31]. This material is currently out of stock. Instead, we obtained IAEA-330, a Spinach sample collected from Polesskoe, Ukraine. The two sites are approximately equidistant (300 km) from the Chernobyl site. We expect the two reference materials to share the same $^{135}Cs/^{137}Cs$ atom ratio and accordingly, IAEA-330 to be a suitable reference material in place of IAEA-375 to validate the proposed methodology. Isotopic measurements of Cs in environmental samples collected from Iitate, Japan have also been published elsewhere [29]. Therefore, roadside dust collected from Iitate, Japan (^{137}Cs activity on 11/03/2011 = 661 ± 49 Bq g^{-1}), has been used as a reference to assess the accuracy of $^{134}Cs/^{137}Cs$ measurements by mass spectrometry in addition to $^{135}Cs/^{137}Cs$ measurements.

The results obtained by this work are in good statistical agreement with the values reported in the literature for both IAEA-330 and Fukushima roadside dust (Table 6). This demonstrates the proposed method is suitable for the determination of $^{135}Cs/^{137}Cs$ atom ratios in a range of environmental samples. Furthermore, it was also possible to obtain $^{134}Cs/^{137}Cs$ atom ratios from the Fukushima roadside dust (Fig. A4). Although $^{134}Cs/^{137}Cs$ may be quantified by gamma-spectrometry, for samples where ^{133}Cs is relatively low, mass spectrometry may offer improved limits of detection and greater precision.

Table 6
$^{134}Cs/^{137}Cs$ and $^{135}Cs/^{137}Cs$ atom ratios measured for Chernobyl and Fukushima derived materials. Uncertainties estimated to 2SE.

Reference	$^{134}Cs/^{137}Cs$ atom ratio	$^{135}Cs/^{137}Cs$ atom ratio
Chernobyl – decay corrected to 26.04.1986		
This study[b]	n/a	0.29 ± 0.02 (n = 3)
Taylor et al. [12][a]	n/a	0.30 ± 0.03 (n = 3)
Zheng et al. [31][a]	n/a	0.29 ± 0.01 (n = 3)
Snow et al. [26][a]	n/a	0.30 ± 0.01 (n = 5)
Zheng et al. [32][b]	n/a	0.29 ± 0.02 (n = 4)
Snow et al. [11][b]	n/a	0.29 ± 0.01 (n = 2)
Iitate village, Fukushima – decay corrected to corrected 11.03.2011		
This study	0.072 ± 0.002 (n = 5)	0.362 ± 0.001 (n = 5)
Shibahara et al. [29]	0.07131 ± 0.0004	0.3625 ± 0.0007

[a] IAEA-375.
[b] IAEA-330.

3.5. Challenges of measuring $^{135,\ 137}Cs/^{133}Cs$ at high dynamic ranges ($< 1 \times 10^{-8}$)

The $^{135,\ 137}Cs/^{133}Cs$ in the Fukushima samples and IAEA-330 were on the order of 1×10^{-6} and 1×10^{-7}, respectively. Notably, at $^{135,\ 137}Cs/^{133}Cs \approx 1 \times 10^{-6}$, scattered $^{133}Cs^+$ does not appear as a significant spectral interference (Fig. A4). However, one of the principal motivations of this study was to establish a routine protocol to quantify $^{135}Cs/^{137}Cs$ atom ratios in environmental samples with $^{135,\ 137}Cs/^{133}Cs \approx 1 \times 10^{-9}$ so that it may be widely used as a forensic tool for nuclear operations and tracing environmental processes. To test our ability to accurately determine atoms ratios, one would normally rely on certified reference materials or commonly-used standards. Unfortunately, such materials do not exist with such a high dynamic range. Instead, we use the three sample splits from homogenized estuarine sediment, which were treated independently through chemistry and mass spectrometry (Fig. 7).

Due to spectral interferences from scattered $^{133}Cs^+$, a mass scan is not an effective means of assessing the presence of interferences at *m/z* 135 and *m/z* 137. To identify potential interfering species with different ionization behavior to Cs, we measured isotope ratios for each sample at a range of filament currents and beam intensities (7 – 110 V $^{133}Cs^+$). No shift in results is apparent for *m/z* 135/^{133}Cs, but shifts of ~ 10% and ~ 30% can be seen for *m/z* 137/^{133}Cs in two of the runs (Fig. 7). These data are sensitive to minor interferences because beam intensities at *m/z* 137 are from 3 to 30 cps.

It is not possible for ^{137}Ba to be the cause of the shift exhibited in Fig. 7 because the proportion of Ba ionized with respect to Cs will increase with filament temperature and therefore, *m/z* 137/^{133}Cs would also increase. Additionally, one would also see a corresponding shift in *m/z* 135/^{133}Cs because of the presence of ^{135}Ba. One or more, as yet unidentified, organic polyatomic interferences discussed earlier is likely to be responsible for the minor interference, with maximum intensity of < 2 cps.

For runs exhibiting a shift in ratio with intensity, we based our mean estimate of *m/z* 137/^{133}Cs atom ratios on the highest intensity data points (upper 25%). In treating the data this way, the $^{135}Cs/^{137}Cs$ atom ratios obtained for the three sample splits show excellent reproducibility at good precision (< 5% 2 SE) considering the challenges these samples present (Fig. 7).

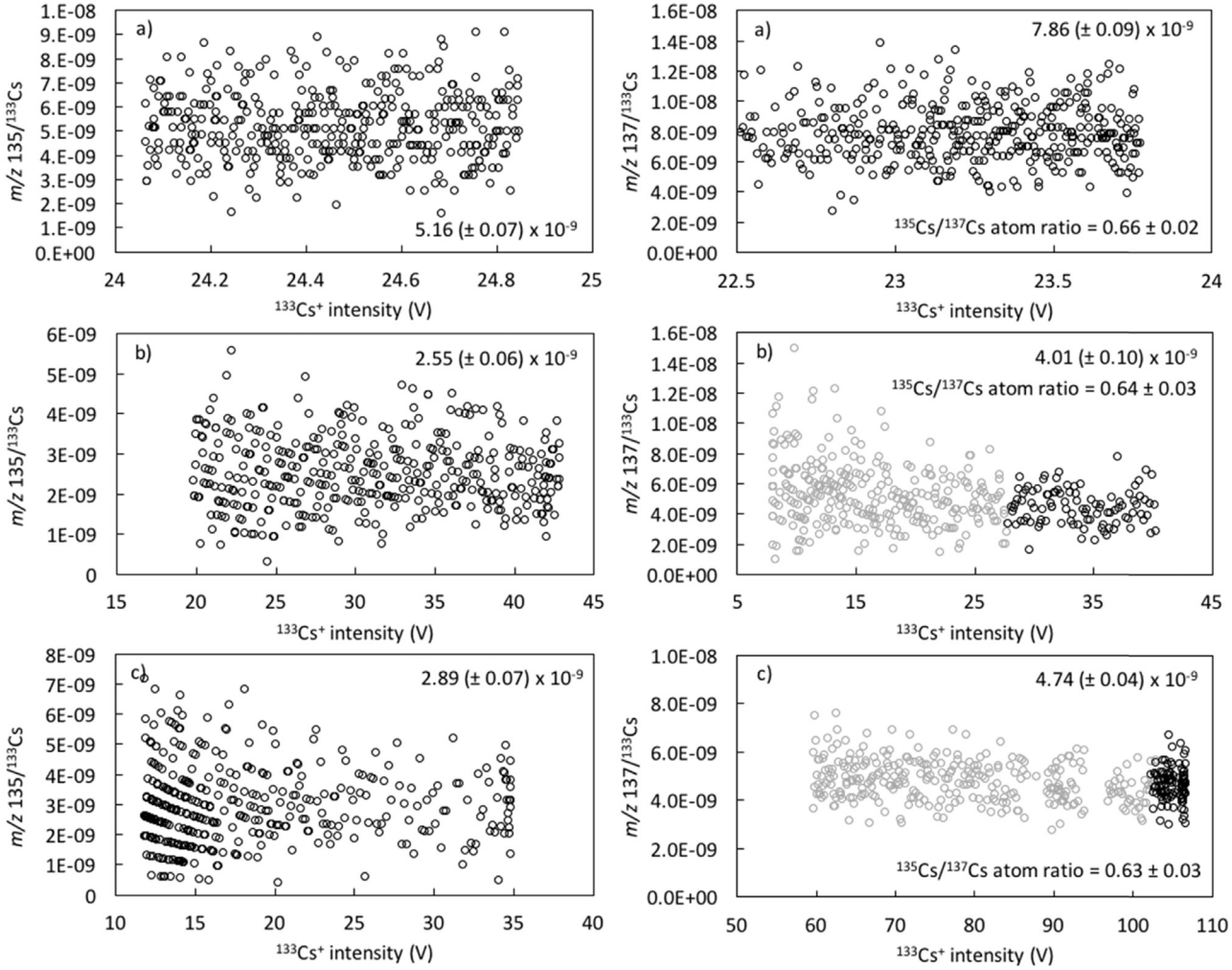

Fig. 7. m/z 135/^{133}Cs and m/z 137/^{133}Cs vs $^{133}Cs^+$ intensity for three samples (a), b), c)) of the same homogenized estuarine sediment sample. For measurements that exhibit statistically significant drift, only the highest (upper 25%) intensity data points (black symbols) have been selected to calculate mean atom ratios. Uncertainties estimated to 2SE.

We consider the reproducibility presented above to show great potential in our methods to quantify ^{135}Cs/^{137}Cs atom ratios in analytically challenging materials where ^{137}Cs concentration is as low as 12 fg g^{-1}. To further confirm the capability of this technique to quantify trace amounts of radiocaesium at the $^{135,\ 137}$Cs/^{133}Cs = 1 × 10^{-9} level, it is recommended that a well-known ^{135}Cs/^{137}Cs standard is diluted with ^{133}Cs.

4. Conclusions

The proposed methodology effectively separates Cs from a range of analytically challenging environmental samples (sediments, soil and spinach). The chemical separation protocol provides excellent separation from species that can potentially be problematic for analysis of Cs isotopes by TIMS (alkali metals, Ba and organic species). A double AMP-PAN anion-exchange column followed by Sr-resin has been shown to provide a larger separation factor from Rb than other values that are reported in the literature (> 600) [26]. This method is used to remove Ba as an isobaric interference because, when adequately separated from the other alkali metals, Cs is ionized at a lower temperature than Ba. These ionization conditions eliminate the requirement to correct for trace Ba interferences, improving measurement precision.

Glucose has been identified as a suitable activator, for a single filament ionization source: Cs loaded onto a single filament with no activator did not yield a sufficient enough ionization efficiency to conduct isotope ratio measurements. By improving ionization efficiency greater precisions may be achieved, this is particularly desirable in situations where sample size is limited. Additionally, unlike TaCl + H_3PO_4 and Silica gel + H_3PO_4, a glucose activator did not promote low temperature polyatomic interferences at *m/z's* 134, 135, 136, 137 and 138.

A detailed discussion is provided on the challenges associated with conducting measurements on samples with $^{135,\ 137}$Cs/^{133}Cs as low as 1 × 10^{-9} using MC-TIMS. Specifically, novel experiments have been designed to better understand the behavior of scattered $^{133}Cs^+$ as a spectral interference. Evidently the profile of scattered $^{133}Cs^+$ appears to be a function of $^{133}Cs^+$ intensity and detector geometry. Remarkably, despite setting the deflection and suppressor voltages of the RPQ to their extremes, scattered $^{133}Cs^+$ continued to produce noise on the axial ion counter. We demonstrate that, to the detriment of Faraday cup performance, to perform accurate isotopic measurements of Cs, $^{133}Cs^+$ should be collected in a Faraday cup. Insights into the m/z filtering capability and associatively, limits of the dynamic ranges of these instruments are anticipated to be of value for measurements of other analytically challenging isotopic systems, such as ^{236}U/^{238}U, ^{41}Ca/^{40}Ca, ^{129}I/^{127}I and ^{90}Sr/^{88}Sr.

Values obtained from materials contaminated from the Fukushima and Chernobyl disasters are in good agreement with those published in the literature. Notably, due to the instruments excellent abundance sensitivity, it has been possible to quantify ^{134}Cs/^{137}Cs atom ratios by mass spectrometry. Similarly, the ^{134}Cs/^{137}Cs atom ratios measured

are in good agreement with other values from Fukushima material. While it is possible to quantify this ratio by gamma-spectrometry, which is generally less labor-intensive, mass spectrometry potentially offers lower limits of detection and greater precision.

Finally, the proposed method was applied to estuarine sediments containing ~ 12 fg g^{-1} of ^{137}Cs, high quantities of alkali metals and Ba and $^{135,\ 137}Cs/^{133}Cs \approx 1 \times 10^{-9}$. Three 1 g sub-samples of homogenized sediment were treated separately through chemistry and subsequently measured by MC-TIMS. These measurements exhibited some evidence of polyatomic interferences. However, by selecting the highest intensity data points, the three samples showed good statistical agreement. This demonstrates the potential of this method to reproducibly quantify $^{135}Cs/^{137}Cs$ atom ratios in ultra-trace quantities at extreme dynamic ranges.

Acknowledgements

We kindly acknowledge invaluable assistance from Drs. Chris Coath, Ian Parkinson and Dan Nita, Bristol Isotope Group. Prof. Yamashiki Yosuke (Kyoto University), Peter Martin and Prof. Tom Scott (Interface Analysis Centre, University of Bristol) provided logistical support for provision of the roadside dust samples from Iitate. Prof. Neil Willey and associates (University of the West of England) provided facilities for gamma-spectrometry measurements. This paper has benefitted from the useful suggestions of two anonymous reviewers. This research was funded by a Natural Environment Research Council (NERC) doctoral training grant (NE/K500823/1).

Appendix A. Supporting information

Supplementary data associated with this article can be found in the online version at doi:10.1016/j.talanta.2017.06.033.

References

[1] S.M. Wright, B.J. Howard, P. Strand, T. Nylén, M.A.K. Sickel, Prediction of ^{137}Cs deposition from atmospheric nuclear weapons tests within the Arctic, Environ. Pollut. 104 (1999) 131–143.
[2] M. Aoyama, K. Hirose, Y. Igarashi, Re-construction and updating our understanding on the global weapons tests ^{137}Cs fallout, J. Environ. Monit. 8 (2006) 431–438.
[3] M. Kohno, Y. Koizumi, K. Okumura, I. Mito, Distribution of environmental Cesium-137 in tree rings, J. Environ. Radioact. 8 (1988) 15–19.
[4] P. Schuller, G. Voigt, J. Handl, A. Ellies, L. Oliva, Global weapons' fallout ^{137}Cs in soils and transfer to vegetation in south-central Chile, J. Environ. Radioact. 62 (2002) 181–193.
[5] P.G. Appleby, Three decades of dating recent sediments by fallout radionuclides: a review, Holocene 18 (2008) 83–93.
[6] Q. He, D.E. Walling, Interpreting particle size effects in the adsorption of ^{137}Cs and unsupported ^{210}Pb by mineral soils and sediments, J. Environ. Radioact. 30 (1996) 117–137.
[7] F. Zapata, The use of environmental radionuclides as tracers in soil erosion and sedimentation investigations: recent advances and future developments, Soil Tillage Res. 69 (2003) 3–13.
[8] D.E. Walling, Q. He, Use of cesium-137 as a tracer in the study of rates and patterns of floodplain sedimentation, Tracers Hydrol. (1993) 319–328.
[9] M.E. Ketterer, K.M. Hafer, V.J. Jones, P.G. Appleby, Rapid dating of recent sediments in Loch Ness: inductively coupled plasma mass spectrometric measurements of global fallout plutonium, Sci. Total Environ. 322 (2004) 221–229.
[10] G. Yang, H. Tazoe, M. Yamada, ^{135}Cs activity and $^{135}Cs/^{137}Cs$ atom ratio in environmental samples before and after the Fukushima Daiichi Nuclear Power Plant accident, Sci. Rep. 6 (2016) 24119.
[11] M.S. Snow, D.C. Snyder, $^{135}Cs/^{137}Cs$ isotopic composition of environmental samples across Europe: environmental transport and source term emission applications, J. Environ. Radioact. 151 (2016) 258–263.
[12] V.F. Taylor, R.D. Evans, R.J. Cornett, Preliminary evaluation of $^{135}Cs/^{137}Cs$ as a forensic tool for identifying source of radioactive contamination, J. Environ. Radioact. 99 (2008) 109–118.
[13] D.C. Snyder, J.E. Delmore, T. Tranter, N.R. Mann, M.L. Abbott, J.E. Olson, Radioactive cesium isotope ratios as a tool for determining dispersal and redispersal mechanisms downwind from the Nevada Nuclear Security Site, J. Environ. Radioact. 110 (2012) 46–52.
[14] J.M. Schwantes, C.R. Orton, R.A. Clark, Analysis of a nuclear accident: fission and activation product releases from the fukushima daiichi nuclear facility as remote indicators of source identification, extent of release, and state of damaged spent nuclear fuel, Environ. Sci. Technol. 46 (2012) 8621–8627.
[15] S.R. Aston, D.A. Stanners, The determination of estuarine sedimentation rates by $^{134}Cs/^{137}Cs$ and other artificial radionuclide profiles, Estuar. Coast. Mar. Sci. 9 (1979) 529–541.
[16] P. Kershaw, A. Baxter, The transfer of reprocessing wastes from north-west Europe to the Arctic, Deep Sea Res. Part II Top. Stud. Oceanogr. 42 (1995) 1413–1448.
[17] P. Bailly du Bois, P. Guéguéniat, Quantitative assessment of dissolved radiotracers in the English Channel: sources, average impact of la Hague reprocessing plant and conservative behaviour (1983, 1986, 1988, 1994), Cont. Shelf Res. 19 (1999) 1977–2002.
[18] J.J.G. Zwolsman, G.W. Berger, G.T.M. Van Eck, Sediment accumulation rates, historical input, postdepositional mobility and retention of major elements and trace metals in salt marsh sediments of the Scheldt estuary, SW Netherlands, Mar. Chem. 44 (1993) 73–94.
[19] Nuclear Decomissioning Authority, Geological Disposal Generic Post-closure Safety Assessment, NDA Report no. NDA/RWMD/030 126, 2010.
[20] S. Asai, Y. Hanzawa, K. Okumura, N. Shinohara, J. Inagawa, S. Hotoku, K. Suzuki, S. Kaneko, Determination of ^{79}Se and ^{135}Cs in Spent Nuclear Fuel for Inventory Estimation of High-Level Radioactive Wastes, J. Nucl. Sci. Technol. 48 (2011) 851–854.
[21] A.C. Hayes, G. Jungman, Determining reactor flux from xenon-136 and cesium-135 in spent fuel, Nucl. Instrum. Methods Phys. Res. Sect. A Accel. Spectrometers, Detect. Assoc. Equip. 690 (2012) 68–74.
[22] M.S. Snow, D.C. Snyder, J.E. Delmore, Fukushima Daiichi reactor source term attribution using cesium isotope ratios from contaminated environmental samples, Rapid Commun. Mass Spectrom. 30 (2016) 523–532.
[23] H.W. Chen, T. Lee, T.L. Ku, J.P. Das, Production ratio of nuclear fallout $^{137}Cs/^{135}Cs$, Chin. J. Phys. 46 (2008) 560–569.
[24] T. Lee, T. Ku, H. Lu, J. Chen, First detection of fallout Cs-135 and potential applications of $^{137}Cs/^{135}Cs$ ratios, Geochim. Cosmochim. Acta 57 (1993) 3493–3497.
[25] M.S. Snow, D.C. Snyder, S.B. Clark, M. Kelley, J.E. Delmore, ^{137}Cs activities and $^{135}Cs/^{137}Cs$ isotopic ratios from soils at idaho national laboratory: a case study for contaminant source attribution in the vicinity of nuclear facilities, Environ. Sci. Technol. 49 (2015) 2741–2748.
[26] M.S. Snow, D.C. Snyder, N.R. Mann, B.M. White, Method for ultra-trace cesium isotope ratio measurements from environmental samples using thermal ionization mass spectrometry, Int. J. Mass Spectrom. (2015) 1–8.
[27] G. Yang, H. Tazoe, M. Yamada, Rapid determination of ^{135}Cs and precise $^{135}Cs/^{137}Cs$ atomic ratio in environmental samples by single-column chromatography coupled to triple-quadrupole inductively coupled plasma-mass spectrometry, Anal. Chim. Acta 908 (2016) 177–184.
[28] L. Cao, J. Zheng, H. Tsukada, S. Pan, Z. Wang, K. Tagami, S. Uchida, Simultaneous determination of radiocesium (^{135}Cs, ^{137}Cs) and plutonium (^{239}Pu, ^{240}Pu) isotopes in river suspended particles by ICP-MS/MS and SF-ICP-MS, Talanta 159 (2016) 55–63.
[29] Y. Shibahara, T. Kubota, T. Fujii, S. Fukutani, T. Ohta, K. Takamiya, R. Okumura, S. Mizuno, H. Yamana, Analysis of cesium isotope compositions in environmental samples by thermal ionization mass spectrometry – 1. A preliminary study for source analysis of radioactive contamination in Fukushima prefecture, J. Nucl. Sci. Technol. 51 (2014) 575–579.
[30] Y. Shibahara, T. Kubota, T. Fujii, S. Fukutani, K. Takamiya, M. Konno, S. Mizuno, H. Yamana, Analysis of cesium isotope compositions in environmental samples by thermal ionization mass spectrometry – 3. Measurement of isotopic ratios of Cs in soil samples obtained in Fukushima prefecture, J. Nucl. Sci. Technol. 51 (2016) 575–579.
[31] J. Zheng, K. Tagami, W. Bu, S. Uchida, Y. Watanabe, Y. Kubota, S. Fuma, S. Ihara, $^{135}Cs/^{137}Cs$ isotopic ratio as a new tracer of radiocesium released from the Fukushima nuclear accident, Environ. Sci. Technol. 48 (2014) 5433–5438.
[32] J. Zheng, L. Cao, K. Tagami, S. Uchida, Triple-quadrupole inductively coupled plasma-mass spectrometry with a high-efficiency sample introduction system for ultratrace determination of ^{135} Cs and ^{137} Cs in environmental samples at femtogram levels, Anal. Chem. 88 (2016) 8772–8779.
[33] B.C. Russell, I.W. Croudace, P.E. Warwick, J.A. Milton, Determination of precise $^{135}Cs/^{137}Cs$ ratio in environmental samples using sector field inductively coupled plasma mass spectrometry, Anal. Chem. 86 (2014) 8719–8726.
[34] J. Gray, S.R. Jones, A. Smith, Discharges to the environment from the Sellafield Site, 1951–1992, J. Radiol. Prot. 15 (1995) 99–131.
[35] J.S. Oh, P.E. Warwick, I.W. Croudace, Spatial distribution of ^{241}Am, ^{137}Cs, ^{238}Pu, $^{239,240}Pu$ and ^{241}Pu over 17 year periods in the Ravenglass saltmarsh, Cumbria, UK, Appl. Radiat. Isot. 67 (2009) 1484–1492.
[36] J. Lehto, H. Xiaolin, Chemistry and Analysis of Radionuclides, WILEY-VCH Verlag & Co. KGaA, Weinheim, 2011.
[37] B.Y.J. Aveston, E.W. Anacker, J.S. Johnson, Hydrolysis of Molybdenum (VI). Ultracentrifugation, acidity measurements, and Raman spectra of polymolybdates, Inorg. Chem. 3 (1964) 735–746.
[38] P.J. Potts, A Handbook of Silicate Rock Analysis, Springer Science & Business Media, Blackie Chapman and Hall, New York, 1989.
[39] J. Van, R. Smit, Ammonium salts of the heteropolyacids as cation exchangers, Nature 181 (1958) 1530–1531.
[40] A. Nobel, AG 50W and AG MP-50 Cation Exchange Resins Instruction Manual, Bio-Rad Laboratories, Hercules, CA, 2000, p. 29.
[41] A.J. Fuller, S. Shaw, M.B. Ward, S.J. Haigh, J.F.W. Mosselmans, C.L. Peacock, S. Stackhouse, A.J. Dent, D. Trivedi, I.T. Burke, Caesium incorporation and retention in illite interlayers, Appl. Clay Sci. 108 (2015) 128–134.
[42] I. Croudace, P. Warwick, R. Taylor, S. Dee, Rapid procedure for plutonium and uranium determination in soils using a borate fusion followed by ion-exchange and

extraction chromatography, Anal. Chim. Acta 371 (1998) 217–225.
[43] S. Bürger, L.R. Riciputi, S. Turgeon, D. Bostick, E. McBay, M. Lavelle, A high efficiency cavity ion source using TIMS for nuclear forensic analysis, J. Alloy. Compd. 444–445 (2007) 660–662.
[44] L. Pibida, C.A. McMahon, B.A. Bushaw, Laser resonance ionization mass spectrometry measurements of cesium in nuclear burn-up and sediment samples, Appl. Radiat. Isot. 60 (2004) 567–570.
[45] C. Gerling, V. Heyd, A. Pike, E. Bánffy, J. Dani, Identifying kurgan graves in Eastern Hungary: a burial mound in the light of strontium and oxygen isotope analysis, Popul. Dyn. Prehistory Early Hist. (2012) 165–176.
[46] S. Triantaphyllou, E. Nikita, T. Kador, Exploring mobility patterns and biological affinities in the Southern Aegean: first insights from early bronze age Eastern Crete, Annu. Br. Sch. Athens (2015) 1–23.
[47] G. Kessinger, J. Delmore, High temperature chemistry of molten glass ion emitters, Int. J. Mass Spectrom. 213 (2002) 63–80.
[48] X. Hou, W. Zhou, N. Chen, L. Zhang, Q. Liu, M. Luo, Y. Fan, W. Liang, Y. Fu, Determination of ultralow level $^{129}I/^{127}I$ in natural samples by separation of microgram carrier free iodine and accelerator mass spectrometry detection, Anal. Chem. 82 (2010) 7713–7721.
[49] F. Arslan, M. Behrendt, W. Ernst, E. Finck, G. Greb, F. Gumbmann, M. Haller, S. Hofmann, R. Karschnick, M. Klein, W. Kretschmer, J. Mackiol, G. Morgenroth, C. Pagels, M. Schleider, Trace analysis of the Radionuclides $9^{0S}r$ and $8^{9S}r$ in environmental samples II: Accelerator Mass Spectrometry (AMS), Angew. Chem. Int. Ed. Engl. 34 (1995) 183–185.
[50] M.A. Hotchkis, D. Child, D. Fink, G. Jacobsen, P. Lee, N. Mino, A. Smith, C. Tuniz, Measurement of ^{236}U in environmental media, Nucl. Instrum. Methods Phys. Res. Sect. B Beam Interact. Mater. At. 172 (2000) 659–665.
[51] B.A. Bushaw, W. Nortershauser, P. Muller, K. Wendt, Diode-laser-based resonance ionization mass spectrometry of the long-lived radionuclide ^{41}Ca with abundance sensitivity $< 10^{-12}$ sensitivity, J. Radioanal. Nucl. Chem. 247 (2001) 351–356.
[52] L. Halicz, A. Galy, N.S. Belshaw, R.K. O'Nions, High-precision measurement of calcium isotopes in carbonates and related materials by multiple collector inductively coupled plasma mass spectrometry (MC-ICP-MS), J. Anal. At. Spectrom. 14 (1999) 1835–1838.